

# OCEAN INTERNAL WAVES OBSERVED IN THE LOMBOK STRAIT

BY R. DWI SUSANTO,  
LEONID MITNIK,  
AND QUANAN ZHENG

THE INDONESIAN SEAS, with their complex coastline geometry and bathymetry, narrow passages, stratified waters, and strong tidal currents, are favorable places for the generation of intensive ocean internal waves. Internal waves, which occur within the subsurface layers of the ocean where density stratification is strong, are generated when the interface between layers is disturbed. Disturbances are often caused by tidal flow passing over shallow underwater obstacles such as a sill or a shallow ridge. Internal waves are commonly observed in the Lombok Strait, one of the outflow straits of the Indonesian throughflow (ITF) (see Gordon, this issue), which transports water from the Pacific to the Indian Ocean.

John Scott Russell, in the 19<sup>th</sup> century, was the first to observe internal waves (Russell, 1838, 1844). He reported the formation of a single unchanging hump or mound in the shallow waters of the Scottish Canal, which was generated when a towed barge was brought to a sharp halt. Since ancient times, mariners sailing the world's oceans observed internal-wave activity, which manifests itself in the form of bands with increased sea-surface roughness and intensive foaming due to wave breaking (rips). Fedorov and Ginzburg (1992) summarized evidence of internal waves from different sources, including papers from *Marine Weather Log*. Horsburgh (Maury, 1861) and Perry and Schimke (1965) described observations of internal waves near the northern tip of Sumatra (Andaman Sea). However, it took more than half a century to establish the model differential equation used

to describe solitary wave behavior, which is when Korteweg and de Vries (1895) coined the phrase "soliton theory" (the Korteweg-de Vries, or K-dV, equation). Since their pioneer publication, hundreds of papers dealing with soliton theory and its applications have been published. Zabusky and Kruskal (1965) were the first people to use a computer to simulate the K-dV equation to demonstrate the collision of two solitary waves. They concluded that the waves retained their shape and propagation speed after collision. In the current era of satellite observations, some space images of the ocean surface show that solitary internal waves indeed retain their shape after collision, confirming these simulation results. For a comprehensive review of internal wave theory as well as their observation in the Andaman Sea, see Osborne and Burch (1980); a brief discussion of internal wave theory is provided in Box 1.

Disturbances, such as those caused by tidal flow of stratified water over shallow sills, can generate internal waves that propagate along density surfaces. These internal waves are a significant mechanism for the transport of momentum and energy within the ocean (Maxworthy, 1979; Osborne and Burch, 1980; Helfrich and Melville, 1986; Lamb, 1994). Ocean internal waves typically have wavelengths from hundreds of meters to tens of kilometers and periods from several minutes to several hours. Their amplitudes (peak to trough) often exceed 100 m. Orbital motions of the water particles associated with internal waves have the largest radius at the pycnocline depth, which decreases down-

ward and upward from this depth. Tidally generated internal waves are usually nonlinear and occur often in the form of wave packets. The amplitude and distance between waves in a wave packet decreases from the front to the rear.

Since the launching of *Seasat* in 1978, *Almaz-1* in 1991, and *European Remote Sensing Satellite* (ERS-1) in 1991 with a synthetic aperture radar (SAR) on board, a large number of the surface imprints of the small-, meso- and sub-synoptic-scale oceanic and atmospheric phenomena have been detected on SAR images of the sea surface. Oceanic internal solitons vertically displace the thermocline and cause internal currents, with near-surface flow convergence and divergence (Gargett and Hughes, 1972). The latter effects can modulate the sea-surface roughness on small length scales [ $O(1-10\text{ cm})$ ], which can be imaged by radar such as satellite-borne SAR (Alpers, 1985). SAR images of the sea surface can delineate oceanic phenomena such as surface waves, internal waves, eddies, fronts, upwelling, shallow bottom

---

**R. Dwi Susanto** ([dwi@ldeo.columbia.edu](mailto:dwi@ldeo.columbia.edu)) is Senior Staff Associate and Director, Indonesian Research Coordination, Lamont-Doherty Earth Observatory of Columbia University, Palisades, NY, USA. **Leonid Mitnik** is Head, Satellite Oceanography Department, V.I. Il'ichev Pacific Oceanological Institute, Far Eastern Branch, Russian Academy of Sciences, Vladivostok, Russia. **Quanan Zheng** is Senior Research Scientist, Department of Atmospheric and Oceanic Science, University of Maryland, College Park, MD, USA.

## BOX 1. INTERNAL WAVE THEORY IN BRIEF

Vertical stratification in the Lombok Strait can be modeled by a two-layer ocean characterized by a shoaling thermocline. For a two-layer ocean, an oceanic internal wave can be described with a dimensional form of the K-dV equation (Osborne and Burch, 1980)

$$\frac{\partial \eta}{\partial t} + C \frac{\partial \eta}{\partial x} + \alpha \eta \frac{\partial \eta}{\partial x} + \beta \frac{\partial^3 \eta}{\partial x^3} = 0, \quad [1]$$

where  $\eta(x, t)$  is the interface displacement between the two layers from the unperturbed level,  $C$  is the linear phase speed,  $\alpha$  is a nonlinear coefficient, and  $\beta$  is the dispersion coefficient. Under certain conditions, the nonlinear term ( $\alpha\eta\eta_x$ ) and the dispersive term ( $\beta\eta_{xxx}$ ) balance. When these terms balance, the result is a stable configuration of a solitary wave, which is a special solution of the K-dV equation and has the analytical solution in the form of

$$\eta = \eta_0 \operatorname{sech}^2 \left[ \frac{(x - Vt)}{\Delta} \right], \quad [2]$$

where  $\eta_0$  is the maximum soliton amplitude,  $V$  is the soliton phase speed, and  $\Delta$  is the characteristic length or half width.

If we know the ocean stratification in the generation and propagation areas, we can calculate the propagation phase speed, soliton amplitude in the interface, characteristic half width, and horizontal velocity of the water particles of soliton in the upper and lower layers. The amplitudes of the horizontal velocities in both layers do not decay with depth, but that velocities in the lower layer are opposite in direction to those in the upper layer (Osborne and Burch, 1980).

topography, island wakes, river plumes, biogenic and oil slicks, and atmospheric phenomena such as convective rolls and cells, atmospheric internal waves, land-sea breezes, katabatic winds, and rain cells (Jackson and Apel, 2004). Table 1 provides an overview of SAR satellites beginning with the ERS-1.

Detection of ocean internal waves on airborne and space-borne SAR images can be traced back to the earliest stage of the technology (Elachi and Apel, 1976; Apel and Gonzalez, 1983; Fu and Holt, 1982, 1984). From SAR images, one can directly determine the location and time, wavelength, or separation distance between two consecutive waves; the length of a crest line; the number of solitons in a wave packet; the distance between two consecutive wave packets; and the propagation direction. SAR images can also be used to determine the characteristic half width and amplitude

of ocean internal solitons (Zheng et al., 2001a, 2001b, 2002) as well as to estimate the ocean mixed layer depth (Li et al., 2000). SAR-image time series have been used to analyze internal-wave evolution (Liu et al., 1998).

In general, SAR signatures caused by dynamic phenomena in the tropical and subtropical ocean are more easily identified than those in mid- and high-latitude waters. In the mid and high latitudes, surface waters are exposed to greater average wind speeds than in the tropics and subtropics, which tend to mask the sea-surface expression of internal waves. Thus, SAR images are particularly useful for studying the tropical Indonesian seas.

### LOMBOK STRAIT

The Lombok Strait (Figure 1) separates the Indonesian islands of Bali and Lombok and is an important pathway for Pacific Ocean water to flow into Indian

Table 1. An overview of Synthetic Aperture Radar (SAR) satellites.

Satellite	ERS-1 and ERS-2	RADARSAT	ENVISAT
Sensor	SAR	SAR	ASAR
Launch Date(s)	Jul 17, 1991 Apr 20, 1995	Nov 4, 1995	Mar 1, 2002
Frequency	5.3 GHz	5.3 GHz	5.3 GHz
Wavelength	5.6 cm	5.6 cm	5.6 cm
Polarization <sup>1</sup>	VV	HH	VV, HH, VH, HV
Incidence Angle	20-26°	10-59°	15-45°
Swath Width	100 km	50-500 km	100-405 km
Ground Resolution	25 x 25 m	8 x 100 m	25 x 25 m 150 x 150 m

<sup>1</sup>V and H are vertical and horizontal polarization of SAR signal, respectively. The first letter denotes polarization of transmitting signal. The second letter represents polarization of receiving signal.

Ocean as part of the ITF. In the northern and central strait, there is a deep channel with water depth up to 1400 m. At the southern outlet, Nusa Penida Island divides the strait into two channels. The western channel, Bandung Strait, is shallower. Its water depth is less than 100 m. The eastern channel is deeper and has an east-west running sill along its bottom. The channel serves as a major passage for water exchange from the Indian Ocean into the strait. The latest measurement carried out during the 2005 Indonesian throughflow cruise showed that the sill-crest depth is about 250 m.

The northern part of the Lombok Strait has mixed tides that have a predominantly diurnal cycle (Chong et al., 2000). However, the tide at the sill region is predominantly semi-diurnal; tidal velocity there can exceed 3.5 m/s (Murray and Arief, 1988; Murray et al., 1990). Nonlinear interactions between the semi-diurnal and diurnal tidal components induce a strong tide with a period close to 14 days (Field and Gordon, 1996; Susanto et al., 2000).

Because of the presence of stratified water, rough topography, and strong tidal currents, the Lombok Strait is characterized by intensive internal-wave generation. These waves are detected on ERS-1/2 and RADARSAT SAR and ENVISAT advanced SAR images. Cresswell and Tildesly (1998) showed the existence of internal-wave features in the southern Lombok Strait on the RADARSAT SAR images taken on July 14 and August 7, 1997. Mitnik et al. (2000) and Mitnik and Alpers (2000) observed nonlinear internal wave packets using ERS-1/2 SAR images. They suggested that the nonlinear solitary waves were generated

by tidal currents in the sill area between the islands of Lombok and Nusa Penida and that their estimated propagation velocity was 1.8–1.9 m/s. Susanto et al. (submitted) suggested that internal waves generated in the sill area of the Lombok Strait propagate in three differ-

ent patterns: southward only, northward only, and in both directions. They concluded that background current associated with the ITF, stratification, and tidal conditions control the internal-wave generation and propagation direction in this region.

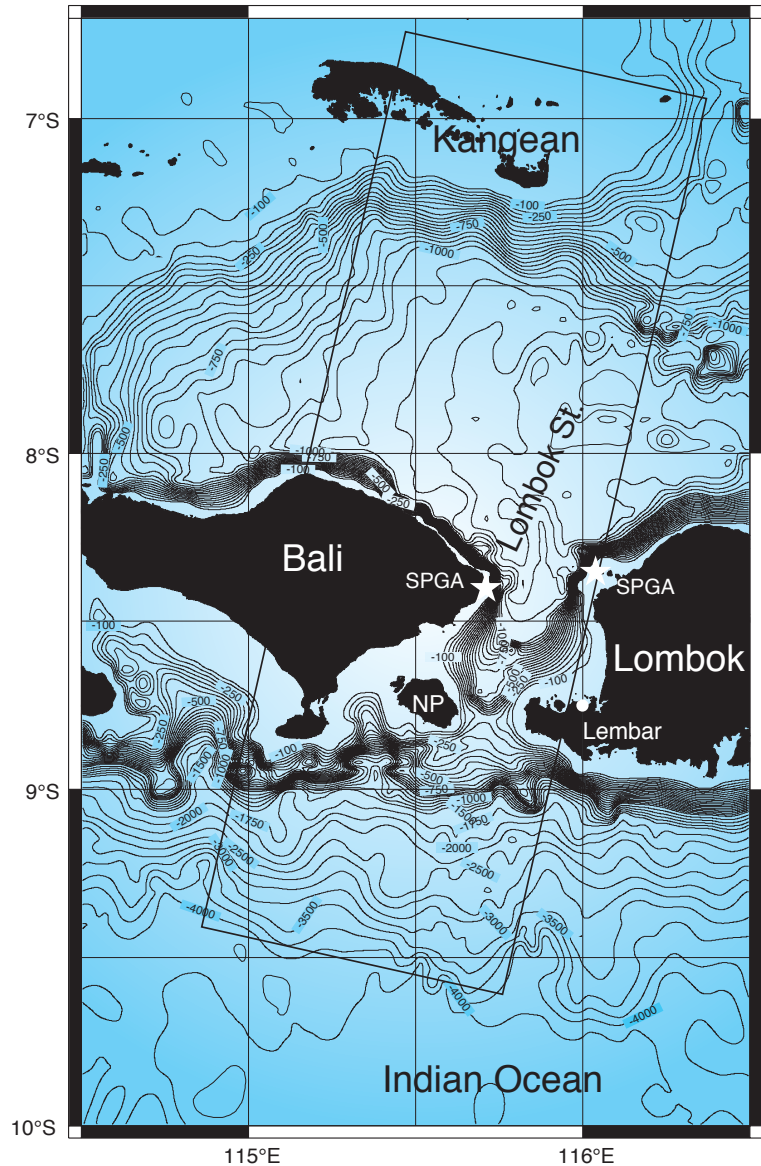
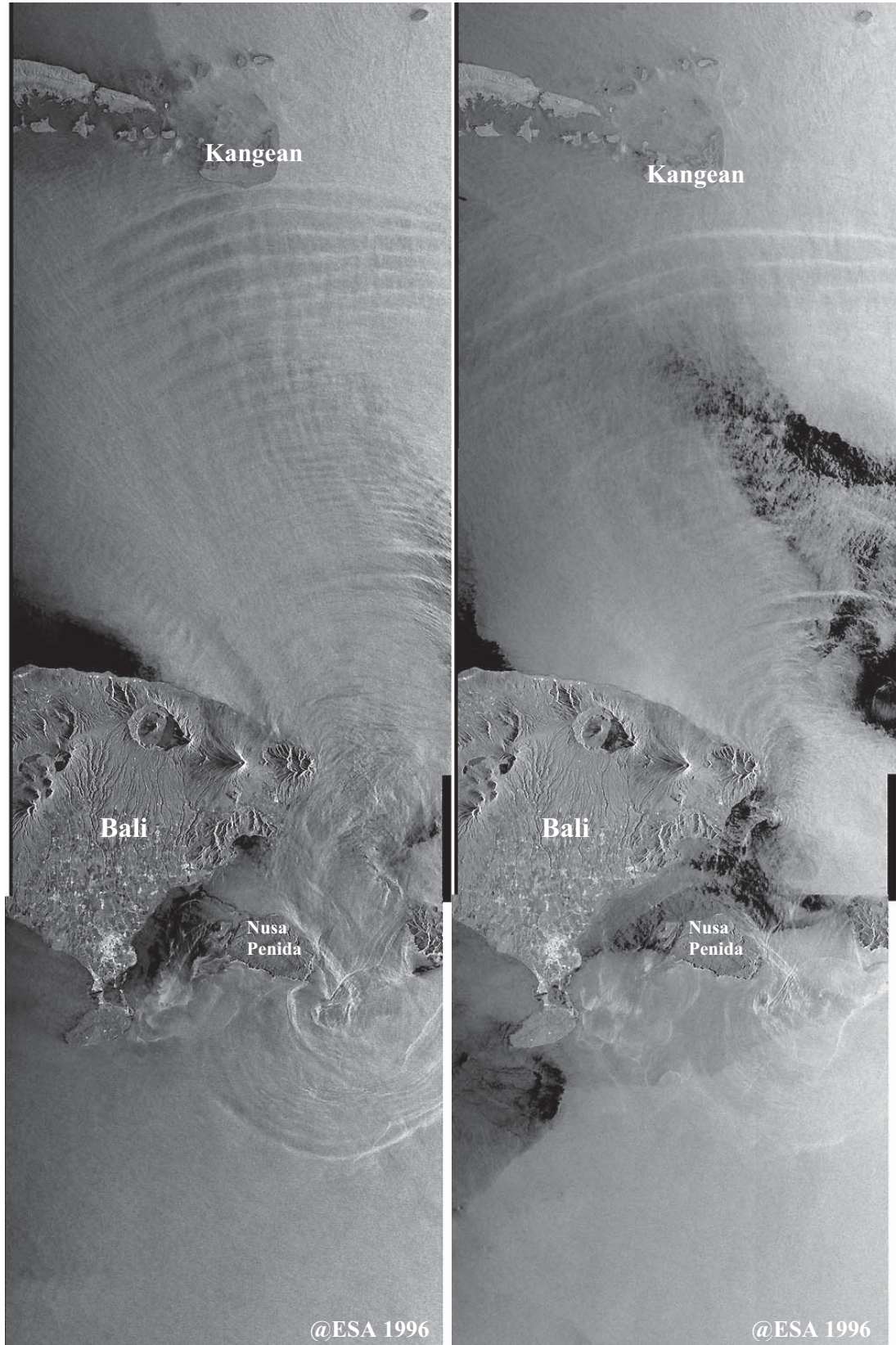


Figure 1. Bathymetry of the Lombok Strait superimposed with the locations of ERS-1/2 SAR images for descending track 418 (solid box). White stars are the locations of shallow pressure gauges (SPGA). The white circle is a tide gauge in Lembar (Lombok). NP is Nusa Penida Island.

Figure 2. SAR images of the Lombok Strait taken at 02:32 UTC on April 23, 1996 by ERS-1 (a) and on April 24, 1996 by ERS-2 (b). Packets of internal solitary waves propagating both northward and southward are clearly seen (circular bright/dark patterns) in both images. Images © the European Space Agency. (a) The northward-propagating internal solitary wave packet contains more than 25 solitons. Wave-packet width is approximately 85 km. The length of crest line of the leading wave exceeds 100 km. Within the wave packet, the wavelengths appear to be monotonically decreasing, from about 5 km in front to 2 km in rear. Three light bands of the second northward propagating packet are clearly seen at middle right. The leading soliton of this packet intrudes the rear of first packet. (b) This image shows radar signature pattern of solitary waves similar to the pattern visible in (a). The crests of the first two solitons are observed within the whole swath width. The wavelength of the first soliton is about 7 km, decreasing to 2 km at the last soliton. The eastern part of the second packet of the northward-propagating solitons has the larger radar contrast due to the decreased brightness of the background within the area of Lombok Island wake (dark northwest-oriented cone area).



## INTERNAL WAVE SIGNATURE ON ERS-1/2 SAR IMAGES

Simultaneous airborne or space-borne SAR sensing and *in situ* measurements can be used to determine generation conditions and propagation direction of internal waves as well as to calculate their dynamic parameters. To estimate characteristics of internal waves in the Lombok Strait, we chose two consecutive images taken during the ERS-1/2 tandem mission (Figure 2). The first image (Figure 2a) was taken by ERS-1 on April 23, 1996 at 02:32 UTC and the second image (Figure 2b) was taken 24 hours later by ERS-2 on April 24. Packets of internal solitary waves propagating both northward and southward are clearly seen in both images. Visibility of solitons (their radar contrast against a background) depends on non-uniformity of sea surface wind conditions, particularly those caused by the interaction of airflow with the high mountains in Bali and Lombok.

The observed internal waves were generated by the interaction of successive tidal flows with the sill between islands of Nusa Penida and Lombok. Based on current measurements using moorings deployed near to the sill, the tidal flow is predominantly semidiurnal (Murray et al., 1990). Hence, by knowing the distance between successive wave packets and their distances to the sill, we can calculate the average wave speed. The distance between packets on the image taken on April 23 is 88.1 km. Meanwhile, on the image taken on April 24, the distance between the consecutive wave packets is 87.6 km. Thus, the average propagation velocity is 1.97 m/s and 1.96 m/s, respectively. Dynamical parameters of these internal waves are

Table 2. Dynamical parameter of northward-propagating internal waves in the Lombok Strait.

Northward Waves	April 23, 1996	April 24, 1996
Solitons in a Packet	25	23
Average Wavelength (Range)	3.10 (2.00–5.00) km	3.80 (2.00–7.25) km
Half Width	$1.99 \pm 0.025$ km	$2.75 \pm 0.025$ km
Mean Phase Speed	$1.97 \pm 0.2$ m/s	$1.96 \pm 0.2$ m/s
First Crest Line Length	> 100 km	> 100 km

summarized in Table 2.

On the SAR image taken on April 23 (Figure 2a), the leading soliton located at the distance of about 180 km from the sill reached the shallow region near the Kangean Island. On the image taken on April 24 (Figure 2b), the distance between the leading soliton and the coral reefs of Kangean Island at the top of the image is 8 km. The difference is mainly due to the fact that the solitons were observed at an earlier phase of the tidal cycle (after two consecutive semidiurnal tides, which is approximately 50 minutes earlier). After accounting for this tidal factor, the leading solitons should have reached 6 km from the Kangean Island. Other factors such as changes in the average background current, tidal conditions, and stratification, which affect wave-propagation speed, are responsible for the 2-km difference.

The southward-propagating internal waves have weaker radar signatures than those propagating northward. About 10 crests are seen on the SAR image (Figure 2a). Their wavelength decreases from about 3 km to 1 km from the front to the rear (from the open water to the strait).

On the second image, taken on the next day (Figure 2b), radar contrast of the southward-propagating internal waves decreased even more. However, the location of the leading soliton can be determined reasonably well on both images. Assuming that the southward propagating packet was generated at the same time as the second northward propagating packet, its speed was approximately a half of the speed of the northward propagating packet. This slower speed indicates that Indian Ocean stratification was different (less intense) from that of the northern Lombok Strait.

The SAR images (Figure 2) were taken after the maximum spring tide. The presence of this tide is evident from analyses of data from shallow pressure-gauge arrays deployed at both sides of the strait (Figure 1) and also tide-gauge data from Lembar (Figure 3). Mixed tide (semidiurnal and diurnal tides) and strong fortnightly tide modulation are clearly seen in Figure 3.

More accurate calculation of dynamic parameters of the solitons requires field observations of the stratification, background currents, and wind and tidal

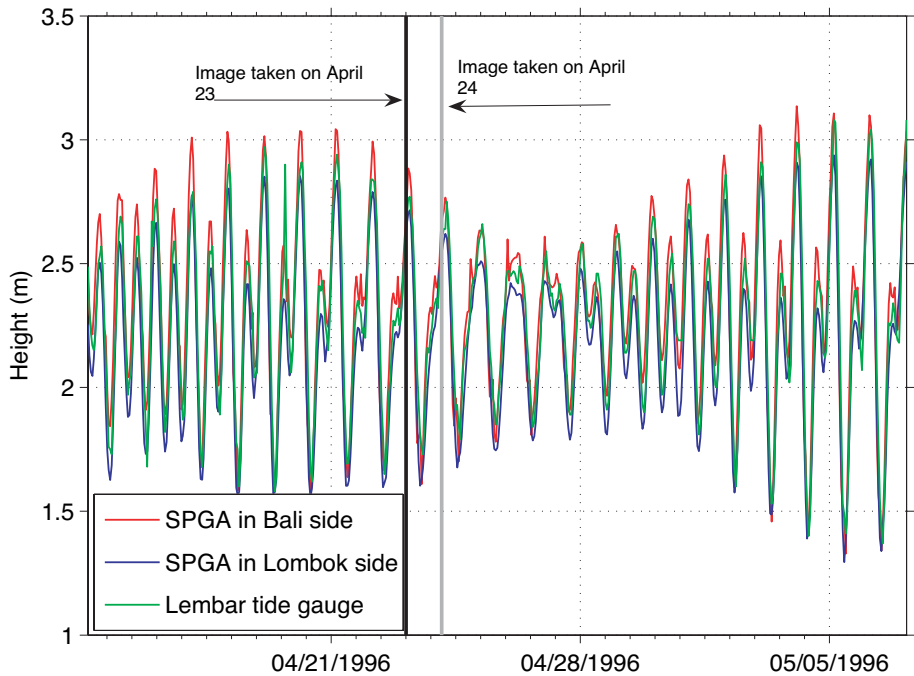


Figure 3. Tidal conditions in the Lombok Strait from April 14 to May 8, 1996. Tidal height was derived from shallow pressure gauges in the Bali side (red) and Lombok side (blue) and from the tidal gauge in Lembar (green). Solid vertical lines mark the time when the images shown in Figure 2 were taken. Mixed tide (semidiurnal and diurnal tides) and strong fortnightly tide modulation are clearly seen. Shallow pressure gauge data are courtesy of Janet Sprintall, Scripps Institution of Oceanography, La Jolla, CA.

conditions collected simultaneously with satellite SAR sensing. Figure 4 provides an example of internal solitary waves propagating northward that was recorded by the ship's echosounder in the Lombok Strait (115.75°E, 8.47°S) during the June/July 2005 INSTANT Indonesian throughflow cruise (see Gordon, this issue). For solitary internal waves, horizontal velocities in the lower layer are opposite in direction to those in the upper layer. Large vertical displacements of water masses (Figure 4) caused by internal waves are important to vertical transport and mixing of biogenic and non-biogenic components in the water column that move nutrients and phytoplankton into or out of the euphotic layer (Weidemann et al., 1996). Intense internal-wave activity, as observed in the Lombok Strait, influences acoustic field properties and undersea navigation.

**SUMMARY**

Lombok Strait is one of the straits in the Indonesian seas where high-amplitude internal solitary waves are observed. The waves are generated in stratified water by interaction among strong tidal flows, background current (i.e., Indonesian throughflow), and rough bottom topography. Analyses of two consecutive satellite SAR images acquired on April 23 and 24, 1996 have shown that internal waves were generated by interaction of successive semidiurnal tidal flows with the sill south of the Lombok Strait. The average propagation speed was 1.96 m/s. Stratification plays an important role in determining the phase speed and amplitude of internal solitary waves. A combination of satellite SAR sensing and field measurements is needed to determine

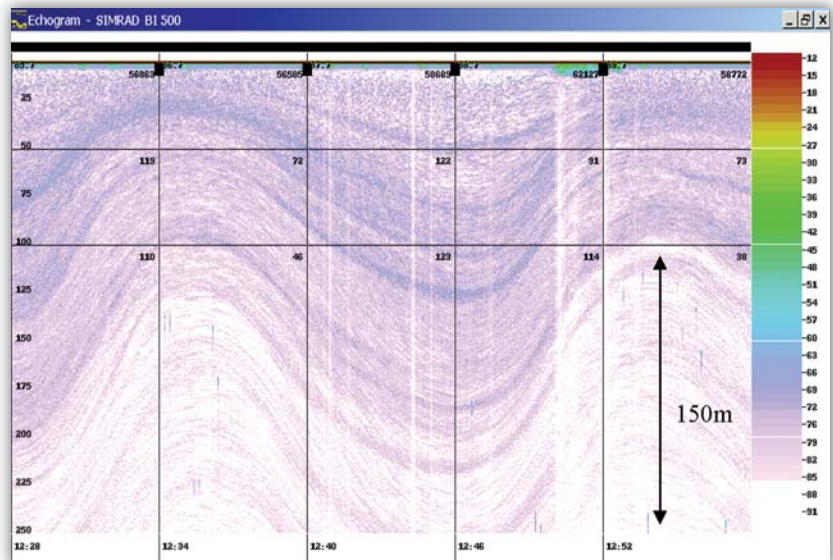


Figure 4. A spectacular echogram of the water column obtained by an EK500 Echosounder operating at frequency of 38 kHz during the 2005 INSTANT Indonesian throughflow cruise. The echogram clearly shows the internal waves in the Lombok Strait. The ship was on standby when waves with a wavelength of ~1.8 km passed under the ship with a speed of ~1.5 m/s. The wave amplitude (peak to trough) exceeds 100 m. Higher backscatter values indicate higher plankton concentration or large schools of fish. Vertical axis is depth in meters. Horizontal axis is time. Colors represent relative backscatter strength in decibels.

the detailed characteristics and dynamics of internal waves and other submesoscale features in the Lombok Strait.

## ACKNOWLEDGEMENTS

This research is funded by the Office of Naval Research (ONR) under grant numbers N00014-04-1-0698, N00014-05-1-0272 and 040611-8331. Leonid Mitnik is partially sponsored by State contract 10002-251/[]-14/197-396/200404-061 (Russia). Lamont-Doherty Earth Observatory Contribution number 6821. 

## REFERENCES

- Alpers, W. 1985. Theory of radar imaging of internal waves. *Nature* 314:245–247.
- Apel, J.R., and F.I. Gonzalez. 1983. Nonlinear features of internal waves off Baja California as observed from the SEASAT imaging radar. *Journal of Geophysical Research* 88:4,459–4,466.
- Chong, J., J. Sprintall, S. Hautala, W. Morawitz, N. Bray, and W. Pandoe. 2000. Shallow throughflow variability in the outflow straits of Indonesia. *Geophysical Research Letters* 27:125–128.
- Cresswell, G., and P. Tildesley. 1998. RADARSAT scenes of Australian and adjacent waters. [Online] available at: [http://www.marine.csiro.au/~cresswell/radarsat\\_paper/](http://www.marine.csiro.au/~cresswell/radarsat_paper/).
- Elachi, C., and J.R. Apel. 1976. Internal wave observations made with an airborne synthetic aperture imaging radar. *Geophysical Research Letters* 3:647–650.
- Fedorov, K.N., and A.I. Ginzburg. 1992. *The Near-Surface Layer of the Ocean*. VSP International Science Publisher, The Netherlands, 256 pp.
- Ffield, A., and A.L. Gordon. 1996. Tidal mixing signatures in the Indonesian Seas. *Journal of Physical Oceanography* 26:1,924–1,937.
- Fu, L.-L., and B. Holt. 1982. Seasat views oceans and sea ice with synthetic aperture radar, *NASA-JPL publication 81-120*. Jet Propulsion Laboratory, California Institute of Technology, Pasadena, CA, USA, 200 pp.
- Fu, L.-L., and B. Holt. 1984. Internal waves in the Gulf of California: Observations from a space borne radar. *Journal of Geophysical Research* 89:2,053–2,060.
- Gargett, A.E., and B.A. Hughes. 1972. On the interaction of surface and internal waves. *Journal of Fluid Mechanics* 52(1):179–191.
- Jackson, C.R., and J.R. Apel. 2004. *Synthetic Aperture Radar Marine User's Manual*, NOAA/NESDIS, Silver Spring, MD, USA, 427 pp.
- Helfrich, K.R., and W.K. Melville. 1986. On long nonlinear internal waves over slope shelf topography. *Journal of Fluid Mechanics* 167:285–308.
- Korteweg, D.J., and G. de Vries. 1895. On the change of long waves advancing in rectangular canal and a new type of long stationary waves. *Philosophical Magazine* 5:422.
- Lamb, K.G. 1994. Numerical experiments of internal wave generation by strong tidal flow across a finite amplitude bank edge. *Journal of Geophysical Research* 99:843–864.
- Li, X., P. Clemente-Colon, and K. S. Friedman. 2000. Estimating oceanic mixed-layer depth from internal wave evolution observed from RADARSAT-1 SAR. *Johns Hopkins APL Technology Digest* 21:130–135.
- Liu, A. K., Y.S. Chang, M.-K. Hsu, and N.K. Liang. 1998. Evolution of nonlinear internal waves in the East and South China Seas. *Journal of Geophysical Research* 103:7,995–8,008.
- Maury, M.F. 1861. *The Physical Geography of the Sea and its Meteorology*, 8<sup>th</sup> ed. Harper & Brothers, New York, NY, 474 pp.
- Maxworthy, T. 1979. A note on the internal solitary wave generation by strong tidal flow over a three-dimensional ridge. *Journal of Geophysical Research* 84:338–346.
- Mitnik, L., W. Alpers, and H. Lim. 2000. Thermal plumes and internal solitary waves generated in the Lombok Strait studied by ERS SAR. Pp. 1–9 in ERS-Envisat Symposium: Looking down to Earth in the New Millennium, 16–20 October 2000. Gothenburg, Sweden. SP-461. European Space Agency, Publication Division, Noordwijk, The Netherlands.
- Mitnik, L., and W. Alpers. 2000. Sea surface circulation through the Lombok Strait studied by ERS SAR. Pp. 313–317 in *Proceedings of the 5<sup>th</sup> Pacific Ocean Remote Sensing Conference (PORSEC 2000)*, Vol. I, 5–8 Dec 2000, Goa, India.
- Murray, S.P., and D. Arief. 1988. Throughflow into the Indian Ocean through Lombok Strait, January 1985–January 1986. *Nature* 333:444–447.
- Murray, S.P., D. Arief, J.C. Kindle, and H.E. Hulburt. 1990. Characteristics of circulation in an Indonesian archipelago strait from hydrography, currents measurements and numerical model results. Pp. 3–23 in *The Physical Oceanography of Straits*, L.J. Pratt, ed. Kluwer Academic Publishers, Norwell, MA, USA.
- Osborne, A.R., and T.L. Burch. 1980. Internal solitons in the Andaman Sea. *Science* 208(4443):451–460.
- Perry, R.B., and G.R. Schimke. 1965. Large amplitude internal waves observed off the northwest coast of Sumatra. *Journal of Geophysical Research* 70:2,319–2,324.
- Russell, J.S. 1838. Report to committee on waves. Pp. 417–496 in *Report of the 7<sup>th</sup> Meeting of the British Association of the Advancement of Science*. British Association of the Advancement of Science, Liverpool, UK.
- Russell, J.S. 1844. Report to committee on waves. Pp. 311–390 in *Report of the 14<sup>th</sup> Meeting of the British Association of the Advancement of Science*. British Association of the Advancement of Science, York, UK.
- Susanto, R.D., Q. Zheng, L. Mitnik, and J. Sprintall. Submitted. Synthetic aperture radar observation of internal waves in the Lombok Strait. *International Journal of Remote Sensing*.
- Susanto, R.D., A.L. Gordon, J. Sprintall, and B. Herunadi. 2000. Intraseasonal variability and tides in Makassar Strait. *Geophysical Research Letters* 27:1,499–1,502.
- Weidemann, A.D., W.S. Pegau, L.A. Jugan, and T.E. Bowers. 1996. Tidal influences on optical variability in shallow water. *Ocean Optics* 2963:320–325.
- Zabusky, N.J., and M.D. Kruskal. 1965. Interaction of solitons in a collisionless plasma and the recurrence of initial states. *Physical Review Letters* 15:243–250.
- Zheng, Q., V. Klemas, X.-H. Yan, and J. Pan. 2001a. Nonlinear evolution of ocean internal solitons as propagating along an inhomogeneous thermocline. *Journal of Geophysical Research* 106:14,083–14,094.
- Zheng, Q., Y. Yuan, V. Klemas, and X.-H. Yan. 2001b. Theoretical expression for an ocean internal soliton SAR image and determination of the soliton characteristic half width. *Journal of Geophysical Research* 106:31,415–31,423.
- Zheng, Q., V. Klemas, and X.-H. Yan. 2002. Advance in studies of ocean internal waves observed from space. In: *Recent Research Developments in Geophysics*. *Research Signpost* 4:143–156.